PORT SAID ENGINEERING RESEARCH JOURNAL
Faculty of Engineering - Port Said University
Volume 29 No. 2 pp: 62:70

Enhancing User Capacity for NOMA Cell-Free Massive MIMO with Carrier Aggregation

*Eslam Ibrahim Khalil [1], Sherif M. Abuelenin [2], Islam E. Shaalan [3, *]*

[1] *Electrical Engineering Department, Faculty of Engineering, Port-Said University, Port-Said, Egypt, email: eslam.ebrahimkhalil @gmail.com*

[2] *Electrical Engineering Department, Faculty of Engineering, Port-Said University, Port-Said, Egypt, email: s.abuelenin@eng.psu.edu.eg*

[3] *Electrical Engineering Department, Faculty of Engineering, Port-Said University, Port-Said, Egypt, email: is_shaalan @eng.psu.edu.eg*

**Corresponding author, DOI: 10.21608/pserj.2025.329397.1373.*

Received 19-10-2024
Revised 6-2-2025
Accepted 17-2-2025

ABSTRACT

Cell-Free Massive Multiple Input Multiple Output (CF-mMIMO) is considered a leading technology to be enrolled in 6G Networks, offering larger capacity which will satisfy the higher rate requirements by the large number of User Equipment (UEs) in next-generation networks, as well as giving better macro-diversity while avoiding inter-cell interference encountered by collocated mMIMO. With Power Domain Non-Orthogonal Multiple Access (PD-NOMA), cell-free massive mimo is expected to support higher capacity for overloaded systems**.** While utilizing PD-NOMA for CF-mMIMO offers more capacity and also better spectrum efficiency compared to the usual Orthogonal Multiple Access (OMA) Cell-Free system, the achievable sum-rate is still limited by the induced interference from users within the same or different clusters leading to lower levels of Signal-to-Interference and Noise Ratio (SINR) at the receiver side. To remedy such a problem, we're going to integrate Carrier Aggregation (CA) into PD-NOMA Cell-Free Massive MIMO system, offering additional frequency bands and thus giving higher rates. Simulation results have shown improvement by a factor of two for the sum-rate, compared to the case when carrier aggregation is not utilized.

Keywords: Cell-Free Massive MIMO, Successive Interference Cancellation, Non-Orthogonal Multiple Access, Carrier Aggregation.

1. INTRODUCTION

1.1 Collocated and Distributed Massive MIMO

Massive Multiple Input Multiple Output (mMIMO) has revolutionized the wireless & mobile communication systems [1–2], for giving a better performance and yet simpler beamforming and coding capability compared to the complex dirty paper coding utilized in Multi-User MIMO [3]. Massive MIMO system can be considered an enhanced version of Multi-User MIMO [1], [4], which relies mainly on beamforming by means of a large number of antenna elements serving a smaller number of users, and thus separating them in spatial domain, giving what is also known as Space Division Multiple Access (SDMA). This separation in spatial domain gives rise to the concept of Favorable Propagation [4–5], where the channels of multiple users become nearly orthogonal, leading to lesser inter-user interference, and thus giving higher spectral efficiency. Massive MIMO has also introduced another advantage to the communication systems, which is Channel Hardening. Channel Hardening [1] is the conversion of the random nature of the propagation channel into a semi-deterministic one, since paths from the transmitted antennas become too

close to each other, leading to smaller fluctuations on the level of the large-scale fading.

Cell-Free Massive MIMO (CF-mMIMO) [6] is regarded as the distributed variant of Massive MIMO system [1] and is predicted to have a greater role in 6G networks [7]. CF-mMIMO uses the same principle of spatial multiplexing which employs a huge number of antenna elements commonly known as Access Points (APs), but instead of being located at the Base Station (BS), they are spread over a wider region giving better signal coverage, lower inter-cell interference and higher macro-diversity, assuming that the number of APs is greater than that of the users or User Equipment (UEs). These APs are connected to a Central Processing Unit (CPU) via a front-haul link (e.g. Optical fiber), which is responsible for exchanging data as well as selecting the power-control coefficients [6]. While CF-mMIMO employs SDMA to separate users' channels, spatial separation becomes challenging when the number of UEs is close to that of APs or even exceeds it, and here comes the role of another multiple access technique which is the Non-Orthogonal Multiple Access (NOMA).

1.2 Non-Orthogonal Multiple Access and CF-mMIMO

Non-Orthogonal Multiple Access (NOMA) [8] is a multiple access technique that permits the transmission of several data streams over the same radio resources and thus allows intentional interference by superimposing several signals over the same resources using superposition coding at the transmitter side, while interference cancellation is utilized at the receiver side to separate them and thus decode the corresponding data stream of each user. Those data streams are multiplexed using power, allowing the transmission or reception of multiple users' data over the same time, frequency or even code resource giving higher capacity and better spectral efficiency compared to its Orthogonal counter-part. NOMA can be classified into two main types: Power-Multiplexed or Power Domain NOMA (PD-NOMA) where Power is utilized to separate users, and Code-Domain NOMA (CD-NOMA) where code is added to power as another dimension for separating users' signals, such as: Sparse Code Multiple Access (SCMA), Pattern Division Multiple Access (PDMA), Interleave Division Multiple Access (IDMA) and Low-Density Spreading (LDS), where coding is used as another dimension to separate users [9] in addition to power.

In PD-NOMA, allocating power to UEs depends on their corresponding path-loss from the Base Station (BS), so that far-UE from BS has higher power relative to its weak channel and near-UE has low power owing to its strong channel, leading to higher inter-user interference resulting from the superimposed users' signals sent over the same channel. Thus, users in NOMA system may encounter three types of interference. The first one is the intra-cluster interference resulting from the contribution of the near-UE signal seen by the far-UE. While such contribution may be assumed as noise and thus neglected, its effect becomes more significant with increasing number of users and also when power difference between signals is reduced. The second type is the imperfect successive interference cancellation (ISIC), where the near-UE needs to decode higher power signal before decoding its own, and so with statistical Channel State Information (CSI), channel estimation becomes inaccurate leading to errors in detecting higher power signals, and therefore, this error propagates to other symbols or signals leading to error propagation and thus imperfect SIC. Another impairment is the inter-cluster interference occurring between different clusters as a result of poor beamforming of the downlink signal from APs.

1.3 Related Works

In [10–11], the authors discussed the combination of NOMA and CF-mMIMO. NOMA has demonstrated to be a good candidate for allowing CF-mMIMO to serve more users over the same allocated resources and thus offer higher capacity while giving better macro-diversity since each UE can receive its signal from a large number of geographically distributed APs. While its OMA counterpart seems to offer a higher achievable sum rate in the regime of the low number of users owing to the intra-cluster pilot contamination and imperfect SIC encountered by NOMA systems, it becomes inefficient when number of UEs approaches that of APs or even exceeds it, making NOMA CF-mMIMO a good choice for massive connectivity systems. Since the inherent interference in the received affects the Signal-to-Interference plus Noise Ratio (SINR) badly, many studies have tried to reduce such effects to help give a boost to the sum-rate.

Several works have studied techniques to minimize such interference. In [12], the authors employed a technique called group-level SIC (GSIC) by dividing users into different groups based on their differences in equivalent path loss, so users in different groups follow the principles of NOMA, and GSIC is used to remove inter-group interference, whereas users within the same group are separated via SDMA. Another contribution was made by the authors of [13], where they tried to improve the achievable sum-rate of the system by introducing cooperative links between UEs by means of short-waves, while also introducing an adaptive switching technique that switches the system between OMA and NOMA. In [14], Raezi et.al has showed the sum-rate of CF-mMIMO system for a number of precoders including conjugate beamformer, zero-forcing, and regularized zero-forcing beamformer. It also showed an improvement in the sum-rate owing to the increasing number of antennas allowing more degrees of freedom (DoF). In [15], the achievable sum-rate is maximized by jointly optimizing the power allocation and user clustering for NOMA CF-mMIMO to

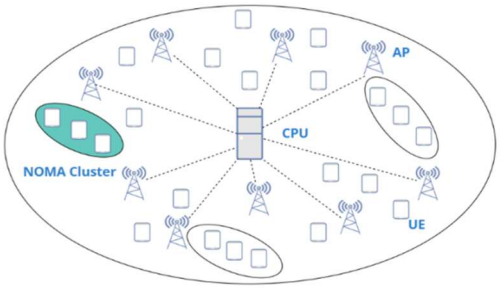

Figure 1: NOMA CF-mMIMO with 3 users per cluster

support Ultra-Reliable Low Latency applications (URLLC).

Another factor that impacts the performance of the NOMA CF-mMIMO is the number of users served per cluster. While the studies [10–15] assume two users per cluster, other studies such as [16–17] showed a NOMA system with larger number of users per cluster. In [16], the author studied the performance of NOMA system in downlink direction assuming three users per cluster and showed the necessary power constraints required for a proper SIC decoding of all users' symbols. In [17], the authors introduced unsupervised machine learning algorithms for user clustering in a NOMA CF-mMIMO system and tried to enhance the system capacity through allowing three users per cluster instead of only two. Motivated by those studies, we're going to assume three UEs per cluster in our system and analyse the system performance accordingly.

1.4 Carrier Aggregation

Carrier Aggregation [18] was introduced to LTE system, to support high-rate data services through combining multiple frequency bands, also known as Component Carriers (CCs), to increase the allocated frequency resources for a system, and thus offering higher rates. Carrier Aggregation (CA) can be classified into three main types according to the position of aggregated CCs with respect to each other: contiguous intra-band, non-contiguous intra-band and inter-band aggregation. In contiguous intra-band, the CCs are adjacent to each other within the same frequency band, whereas in case of non-contiguous aggregation, the aggregated CCs are non-adjacent but within the same band. For the inter-band type, the CCs are located within different frequency bands, and is considered to be difficult to implement [18], since CCs from different frequency bands may require different transceiver chains owing to the frequency separation in between.

CA has been introduced to Massive MIMO systems in [19], to improve the network rate as well as the Energy Efficiency (EE) of the system allowing the reduction of deployed antennas without reducing the rate performance. In [20], CA has been utilized with NOMA system, to offer larger bandwidth and higher data rate for users in Ultra-Dense Network (UDN) system and to circumvent the inherent interference in NOMA resulting from the superimposed signals of various UEs over the same resource.

While the work in [12] tried to enhance the performance of the system and SIC, it didn't give any insights on the achievable sum-rate of the system, and instead showed the effect of the proposed technique GSIC on the transmit power compared to OMA and SIC-NOMA. The cooperative links technique studied in [13], despite giving better sum-rate, it adds more complexity to the system, since it requires an additional channel estimation step for the channel between stronger and weaker UEs exchanging data over the established cooperative links, and also increases power consumption at the user side, requiring the re-transmission of the decoded symbols of farther UEs, degrading the power efficiency. The works in [19] and [20] are more focused on collocated systems, and no analysis has been given to distributed systems such as cell-free networks.

In this study, we're going to take a different approach for improving the achievable rate, by utilizing carrier aggregation method (CA), by extending the allocated frequency band offering higher data rate. The introduction of carrier aggregation (CA) to the PD-NOMA CF-mMIMO system is investigated, and the performance of the system is discussed in light of the added carrier components (CCs) to the system. While integrating carrier-aggregation with NOMA has been discussed before in [20] for Ultra-Dense Networks (UDNs), to the extent of our knowledge, this is the first time to apply such a technique to NOMA CF-mMIMO. This study is organized as follows: Section 2 discusses the system model showing the downlink signal model and achievable sum-rate. Simulation results are discussed in section 3 to show the performance of the proposed for applying carrier aggregation. For readability, Table 1 defines the common symbols used in this study.

Table 1. Table of Symbols

Symbol	Description
$\mathbf{M}$	Number of APs
$\mathbf{K}$	Number of Users per cluster
$\mathbf{N}$	Number of clusters
$\mathbf{P_p}$	Pilot sequence power
$\mathbf{h_{mnk}}$	Channel of k^{th} UE from m^{th} AP over n^{th} cluster
$\boldsymbol{\beta_{mnk}}$	Large-scale fading coefficient
$\boldsymbol{\varphi_{pn}}$	Pilot sequence of n^{th} cluster
$\hat{\mathbf{h}}_{\mathbf{mnk}}$	Estimated Channel of k^{th} UE from m^{th} AP over n^{th} cluster
$\boldsymbol{\gamma_{mnk}}$	Estimated Large-scale fading coefficient
$\boldsymbol{\delta_{mnk}}$	Estimated Small-scale fading coefficient

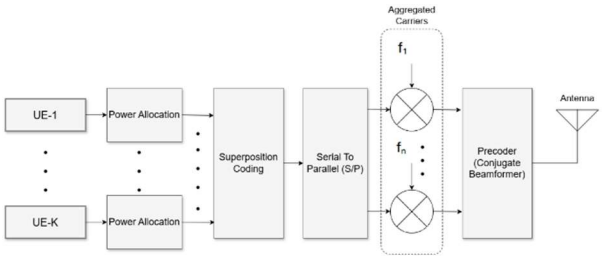

Figure 1: Downlink Signal in NOMA CF-mMIMO with Carrier Aggregation

2. SYSTEM MODEL

2.1 System Model

This system involves an M single-antenna APs distributed randomly to serve a larger number of single-antenna UEs grouped into N-clusters (Fig.1), so that each cluster has K-users.

2.2 Channel Model

The downlink channel h_{mnk} between the mth AP and the kth UE within each nth cluster is represented as shown:

$$h_{mnk} = \sqrt{\beta_{mnk}}\alpha_{mnk} \quad (1)$$

The coefficients β_{mnk} and α_{mnk} are the large scale and small-scale fading coefficients respectively. α_{mnk} is a circularly symmetric complex Gaussian distributed random variable with zero-mean and unit variance $\alpha_{mnk} \sim CN(0,1)$. The large-scale fading (β_{mnk}) is assumed to be known a priori, since it's slowly varying and may be estimated every 40-coherence interval [10–11]. This makes the channel $h_{mnk} \sim CN(0, \beta_{mnk})$ a complex gaussian random variable with zero-mean and variance of β_{mnk}, and accounts for quasi-static Rayleigh fading.

2.3 Uplink Pilot Signal and Channel Estimation

According to [1],[11] each AP uses the uplink pilot signal to estimate the channel to each UE while assuming the existence of channel reciprocity and utilizing Time Division Duplexing (TDD), which permits the estimation of downlink channel. To reduce the overhead of allocating many pilot sequences, the same training sequence is shared among all users within the same cluster, while each cluster takes a unique orthogonal pilot sequence, satisfying the condition $\|\boldsymbol{\varphi_{pn}}\|^2 = \mathbf{1}$ to give the received signal vector as:

$$\boldsymbol{y_{m,p}} = \sum_{n=1}^{N}\sum_{k=1}^{K}\sqrt{\tau P_p}h_{mnk}\boldsymbol{\varphi_{pn}} + \boldsymbol{n_m} \quad (2)$$

Where, $\mathbf{y_{m,p}} \in \mathbf{C^{\tau\times 1}}$ is the uplink pilot signal vector at mth AP representing τ samples of the pilot sequence. P_p, $\boldsymbol{\varphi_{pn}}$, τ and $\mathbf{C^{\tau\times 1}}$ are the pilot power, pilot sequence length, pilot sequence allocated for K users in nth cluster and complex Gaussian random vector with independent and identically distributed (i.i.d) $CN(0_{\tau\times 1}, I_\tau)$, where I_τ is the identity matrix. $\mathbf{n_m}$ is the complex gaussian noise such that $\mathbf{n_m} \in \mathbf{C^{\tau\times 1}}$.

Projecting the uplink signal over the transmitted pilot $\boldsymbol{\varphi_{pn}}$ to get the uplink signal as:

$$\tilde{y}_m^p = \boldsymbol{y_{m,p}}\boldsymbol{\varphi_{pn}^H} = \sum_{n=1}^{N}\sum_{k=1}^{K}\sqrt{\tau P_p}h_{mnk} + \boldsymbol{n_m}\boldsymbol{\varphi_{pn}^H} \quad (3)$$

Applying the MMSE Estimator [21], should give the estimated channel as shown:

$$\hat{h}_{mnk} = \frac{\sqrt{\tau P_p}\beta_{kmn}}{1+\tau P_p\sum_{k=1}^{K}\beta_{kmn}}\tilde{y}_m^p \quad (4)$$

As the signal is gaussian distributed, then the uplink estimated channel can be represented as:

$$\hat{h}_{mnk} = \sqrt{\gamma_{mnk}}\delta_{mnk} \quad (5)$$

where $\delta_{mnk} \in CN(0,1)$ and $\gamma_{mnk} = \frac{\tau P_p \beta_{mnk}^2}{1+\tau P_p \sum_{k=1}^{K}\beta_{kmn}}$ are the estimated large-scale, and small-scale fading coefficients. Channel estimation will be defined as $\epsilon_{mnk} = h_{mnk} - \hat{h}_{mnk}$,where $\epsilon_{mnk} \sim C(0, (\beta_{kmn} - \gamma_{mnk}))$ and thus $Var(\epsilon_{mnk}) = E[|\epsilon_{mnk}|^2] = \beta_{kmn} - \gamma_{mnk}$.

2.4 Beamforming and Downlink Signal Model

In the downlink direction, APs utilize the conjugate beamformer using the locally estimated CSI in the uplink, as shown in fig.(2). The downlink signal is actually the superposition coded symbols of all K-users within the nth cluster, and so we've:

$$x_n = \sum_{k=1}^{K}\sqrt{P_{nk}}x_{nk} \quad (6)$$

Where x_{nk} is the superposed signal over nth cluster, $n \in \{1,2,\dots,N\}$, of the kth user with $k \in \{1,2,\dots,K\}$. Assuming a unity powered data symbol, we should have:

$$E[x_{nk}x_{zk}] = \begin{cases} 1 & n = z, k = j \text{ and } a = b \\ 0 & otherwise \end{cases} \quad (7)$$

Therefore, the transmitted power can be formulated as shown $E[|x_n|^2] = E\left[\left|\sum_{k=1}^{K}\sqrt{P_{nk}}x_{nk}\right|^2\right] = \sum_{k=1}^{K}P_{nk} = P_n$. Using the uplink MMSE channel estimates, we can construct the conjugate beamforming weights to be as shown in (8).

$$w_{mn} = \frac{\hat{h}_{mnk}^{*}}{|\hat{h}_{mnk}^{*}|} = \frac{\delta_{mnk}^{*}}{|\hat{\delta}_{mnk}^{*}|} \quad (8)$$

Since NOMA employs power multiplexing to separate users over the same carrier, then UEs in the same nth cluster are sorted based on the channel strengths as shown:

$$\left|w_{mn}\hat{h}_{mn1}\right| \geq \left|w_{mn}\hat{h}_{mn2}\right| \geq \cdots \geq \left|w_{mn}\hat{h}_{mnK}\right| \quad (9)$$

Thus, the received signal at ith user over nth cluster from all APs should be as shown in (10):

$$y_{nk} = \underbrace{\sum_{m=1}^{M}\sum_{i=1}^{k-1}\sqrt{P_{ni}}w_{mn}h_{mni}x_{ni}}_{\text{Intra-cluster interference}} + \underbrace{\sum_{m=1}^{M}\sum_{i=k+1}^{K}\sqrt{P_{ni}}w_{mn}(h_{mni}x_{ni} - E(h_{mni})\hat{x}_{ni})}_{\text{Imperfect Successive Interference cancellation}} + \underbrace{\sum_{m=1}^{M}\sqrt{P_{nk}}w_{mn}h_{mnk}x_{nk}}_{\text{Desired User signal (k)}} + \underbrace{\sum_{m=1}^{M}\sum_{\substack{n'=1\\ n'\neq n}}^{N}\sqrt{P_{n'}}w_{mn}h_{mn'}x_{n'k}}_{\text{Inter-cluster interference}} + \underbrace{n}_{\text{AWGN}} \quad (10)$$

Assuming that the precoding weights and the channel coefficient can be grouped into $q_{mnk} = \sum_{m=1}^{M} w_{mn}h_{mnk}$, then the simplified form of the received signal will take the form in (11).

$$y_{nk} = \underbrace{\sum_{i=1}^{k-1}\sqrt{P_{ni}}q_{mni}x_{ni}}_{\text{Intra-cluster interference}} + \underbrace{\sum_{i=k+1}^{K}\sqrt{P_{ni}}(q_{mni}x_{ni} - E(q_{mni})\hat{x}_{ni})}_{\text{Imperfect Successive Interference cancellation}} + \underbrace{\sqrt{P_{ni}}q_{mnk}x_{nk}}_{\text{Desired User signal (k)}} + \underbrace{\sum_{\substack{n'=1\\ n'\neq n}}^{N}\sqrt{P_{n'}}q_{mn'k}x_{n'k}}_{\text{Inter-cluster interference}} + \underbrace{n}_{\text{AWGN}} \quad (11)$$

Since statistical CSI is employed at UE, the estimated symbol $\hat{x}_{nk}$ and the actual symbol x_{ni} are jointly gaussian distributed with a correlation coefficient ρnk, as $x_{nm} = \rho\hat{x}_{nk} + e_{nk}$, and $e_{nk} \sim CN\left(0, {\sigma^2_{e_{nk}}}/{1+\sigma^2_{e_{nk}}}\right)$ represents the error between the actual and estimated data symbol and $\rho_{nk} = 1/\sqrt{1+\sigma^2_{enk}}$ is the correlation coefficient between the estimated and actual data symbol.

2.5 Achievable Rate Analysis

Assuming only statistical CSI available to the receiver then, another term appears representing the amount of error introduced by the use of statistical CSI, and therefore, the signal model should be:

$$y_{nk} = \underbrace{\sqrt{P_{nk}}E[q_{mnk}]x_{nk}}_{\text{Desired User signal (i)}} + \underbrace{\sqrt{P_{nk}}\{q_{mnk} - E[q_{mnk}]\}x_{nk}}_{\text{Statistical CSI uncertainty}} + \underbrace{\sum_{i=1}^{k-1}\sqrt{P_{ni}}q_{mni}x_{ni}}_{\text{Intra-cluste interference}} + \underbrace{\sum_{i=k+1}^{K}\sqrt{P_{ni}}(q_{mni}x_{ni} - E(q_{mni})\hat{x}_{ni})}_{\text{Imperfect Successive Interference cancellation}} + \underbrace{\sum_{\substack{n'=1\\ n'\neq n}}^{N}\sqrt{P_{n'}}q_{mn'i}x_{n'i}}_{\text{Inter-cluster interference}} + \underbrace{n}_{\text{AWGN}} \quad (12)$$

Therefore, the Signal-to-Interference plus Noise ratio (SINR) for the statistical CSI case for the k^{th} UE over the n^{th} cluster, should be calculated as shown in (13).

$$SINR_{nk} = \frac{P_1}{\sum_{i=2}^{5} P_i + \sigma_n^2} \quad (13)$$

$$\text{Desired User Signal} \rightarrow P_1 = P_{nk}E[|q_{mnk}|^2] = P_{nk}\left(\sum_{m=1}^{M}\sqrt{\gamma_{mnk}}\right)^2 \quad (13a)$$

$$\text{Statistical CSI Uncertainty} \rightarrow P_2 = P_{nk}E[|q_{mnk} - E(q_{mnk})|^2] = P_n\left[\sum_{m=1}^{M}(\beta_{kmn} - \gamma_{mnk})\right] \quad (13b)$$

$$\text{Intra-cluster interference} \rightarrow P_3 = \sum_{i=1}^{k-1}P_{ni}E[|q_{mni}|^2] = \left(\sum_{m=1}^{M}\sqrt{\gamma_{mnk}}\right)^2\left[\sum_{i=1}^{k-1}P_{ni}\right] \quad (13c)$$

$$\text{Imperfect SIC} \rightarrow P_4 = \sum_{i=k+1}^{K}P_{ni}E[|(q_{mni}x_{ni} - E(q_{mni})\hat{x}_{ni})|^2] = \left(\sum_{m=1}^{M}\sqrt{\gamma_{mnk}}\right)^2\left[\sum_{i=k+1}^{K}P_{ni}(1-2\rho_{ni})\right] \quad (13d)$$

$$\text{Intercluster} \rightarrow P_5 = \sum_{\substack{n'=1\\ n'\neq n}}^{N}P_{n'}E[|q_{mn'k}|^2] = \sum_{\substack{n'=1\\ n'\neq n}}^{N}P_{n'}\left(\sum_{m=1}^{M}\beta_{kmn}\right) \quad (13e)$$

Using (13), the achievable rate of k^{th} user over n^{th} cluster can be calculated using the following formula:

$$R_{nk} = \varphi\log_2(1 + SINR_{nk}) \quad (14)$$

where φ is the pre-log scale factor defined as $\varphi = {\tau_c - \tau}/{\tau_c}$, and τ is the training sequence length. According to the above formula, the achievable sum-rate of the NOMA CF-mMIMO for all clusters over the fth carrier component should be calculated as shown below:

$$R_f = \sum_{n=1}^{N}\sum_{k=1}^{K}R_{nk,f} \quad (15)$$

2.6 Carrier Aggregation for NOMA CF-mMIMO

With intra-band contiguous CA, and using the formula in (15), the achievable sum-rate of the system over all CCs can be approximated to the following formula:

$$R_{CA} \approx \sum_{f=1}^{F} R_f \qquad (16)$$

3. RESULTS AND DISCUSSIONS

This system is assumed to have M APs distributed uniformly within a region having an area of L × L km2 to serve a larger number of UEs grouped into N clusters, each having K users, with L representing the length of the given region. The path-loss model is $\beta_{mnk} = {}^{1}/_{d^{-\alpha}}$ where (d) is the distance between the mth AP and kth UE in the nth cluster, and α is the path-loss exponent [11]. Transmitting powers of AP, and UE are P_{AP} and P_{UE}, respectively. Minimum and Maximum distances between UE and AP are represented as dmin and dmax respectively. The same pilot sequence is shared among all UEs within the same cluster, while mutually orthogonal pilots are utilized between different clusters, with a pilot sequence length of τ_{NOMA} = N, where N is the number of clusters, and for OMA we've τ_{OMA} = KN, and the coherence interval is $\tau_c = 196$ symbols, which is the maximum number of users that can be served simultaneously in OMA system [11]. Noise variance is $\sigma_{ni}^2 = 290 \times k_b \times BW \times NF$, where k_b is Boltzmann's constant, BW is the allocated bandwidth of the system, and NF is the Noise Figure. Power coefficients of UEs are ratios of the power allocated to each UE to the power of cluster Pn, taking the values (0.1 : 0.3 : 0.6). The power of cluster is represented by P_{AP}/N [14]. These power coefficients are not necessarily optimal but can be further optimized. Simulation parameters of this system are mainly set from the works [11], [13], [14], and [15]. The values of the system parameters mentioned in this section are shown in Table 2.

Analytical results of achievable sum-rate in (16) are compared against Monte-Carlo simulated results of the same equation in the given three figures. The simulation tool used to generate such results is MATLAB.

In Fig.(3), the NOMA CF-mMIMO achievable sum-rate is shown for the two cases: two UEs per cluster, and three UEs per cluster. This figure demonstrates that serving three UEs within each cluster offers larger system capacity, but at the expense of higher interference introduced into the system, since UEs with lower power will face increasing imperfect SIC decoding errors from those with higher power levels, and at the same time, introducing more UEs leads to more intra-cluster interference faced by farther UEs from their serving APs, and thus the overall sum-rate is reduced.

Table 2. System Parameters

Parameter	Value
Number of APs M	100
Number of UEs per cluster K	3
Path-loss exponent α	≥ 2
Noise Figure NF	9 dB
Minimum/Maximum distance AP-UE (dmin, dmax)	10 m, 50 m
Coherence Interval τ_c	τc = 196
Transmitting power (P_{AP}, P_{UE})	200 mW, 100 mW
Bandwidth BW	10 MHz
Correlation Coefficient ρ_{ni}	0.1
L	1 km

In Fig.(4), the achievable sum-rate of the system in case of using OMA & NOMA techniques are shown, where three cases are discussed here which are: No Carrier Aggregation (CA), the case of utilizing CA, and NOMA with cooperative links between UEs. The curve with solid line (bottom curve) represents the sum-rate of the NOMA CF-mMIMO system when no CA is used, while the dotted line shows the achievable sum-rate for the case of using cooperative links, and the dashed line above it shows the rate in case of utilizing CA. It's apparent that the utilization of CA is superior to that of cooperative links and offered a higher sum-rate by a factor of two owing to the introduction of an additional carrier component to the system, giving an achievable rate of approximately 16.25 bps/Hz compared to that of 8.13 bps/Hz for the case of no CA, and 9.72 bps/Hz for the case of using cooperative links at 100 simultaneous UEs.

Fig.(5) shows the achievable-sum rate in case of adding two carrier components instead of only one. Aggregating two CCs instead of only one leads to 3x increase of the sum-rate compared to the one without any additional CA, and the overall system performance seems to be improved by the aggregation of multiple CCs to the system bandwidth, which helps compensate for the drop-in rate made by the inherent interference either intra-cluster interference, or imperfect SIC. The dotted line representing the aggregation of two CCs shows a sum-rate of 24.68 bps/Hz at 100 simultaneous UEs. This demonstrates that utilizing CA is much better in terms of the achievable sum-rate compared to the use of cooperative links.

4. CONCLUSION

In this study, we investigated the achievable sum-rate of NOMA CF-mMIMO considering the effects of intra-cluster pilot contamination, inter-cluster interference and imperfect SIC. We also investigated the performance of the NOMA CF-mMIMO with carrier aggregation. It has been demonstrated that the introduction of carrier aggregation to cell-free system can improve the sum-rate of the system, thanks to the extra CCs added to the system, offering higher-rate that can compensate for the reduced performance owing to the inherent interference in the received signal. Simulation results demonstrated an increase in the sum-rate by a factor of two and three respectively.

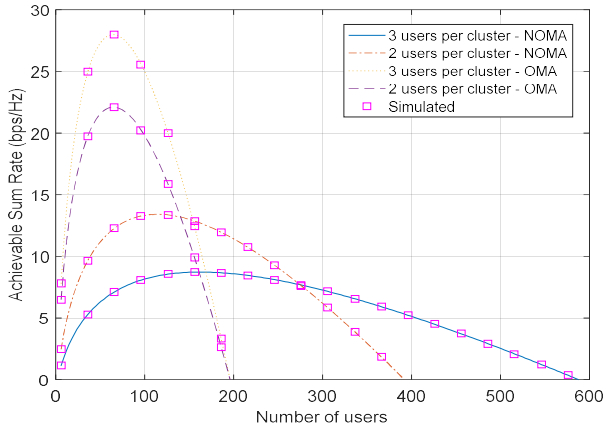

Figure 2: Achievable sum-rate for CF-mMIMO NOMA comparing two & three UEs per cluster.

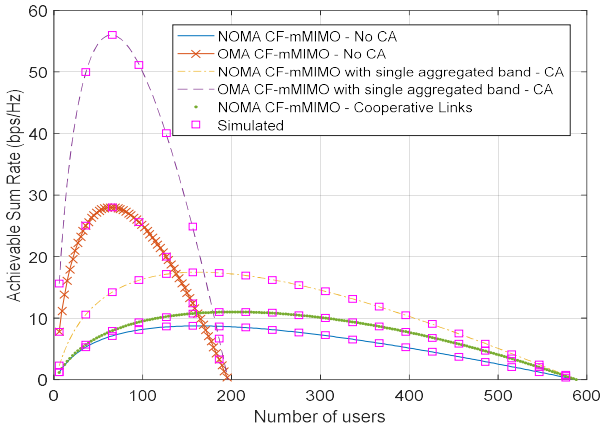

Figure 3: Comparing sum-rate with CA using an extra band giving higher rate owing to the extended bandwidth of the system.

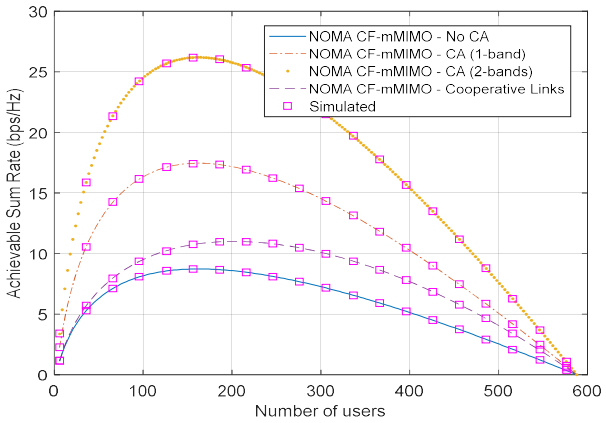

Figure 4: Sum rate of the proposed NOMA CF-mMIMO with adding 2 CCs instead of only a single CC compared to the case with no CA, single aggregated CC, and Cooperative Links.

5. FUTURE WORKS

In our study, we assumed a simplified analysis for a NOMA CF-mMIMO employing intra-band contiguous CA which is considered the simplest type of CA in terms of implementation; however, more analysis is required for other types of CA such as: non-contiguous intra-band CA, and inter-band CA. While CA managed to give a higher achievable rate for the system, it also adds a number of challenges such as: increasing hardware complexity, non-contiguous CA interference management, and variations in channel parameters over different frequency bands. Integrating of CA into CF-mMIMO adds more complexity to the system, requiring power amplifiers, radio frequency chains, and oscillators, which may be costly to integrate into the APs whose power capabilities are limited. Another limitation to the CA technique is the interference resulting from utilizing non-contiguous CA, which arises when mobile phones aggregate carriers across various frequency ranges such as low-band and mid-band. Channel estimation also poses a challenge in CA, specifically when CCs are non-contiguous, since each carrier component is considered a separate channel introducing higher complexity and overhead in channel estimation stage specifically at the user side, which can also worsen when the channel suffers frequency-selective fading.

NOMA CF-mMIMO with CA have a number of implications on 6G networks including: scalability, network deployment, front-haul capacity, and cost efficiency. Some of these challenges have been addressed for CF-mMIMO in [22], however, they may need more extensive study in case of integrating NOMA & Carrier Aggregation together, since CA may add more overhead on the CPUs and thus limit the system scalability. Many studies [6], [11–15] have assumed that all UEs are being served by all APs within the system, which imposes a challenge in making the system unscalable and unrealistic in practice [22], since all APs are required to estimate

channel parameters between them and each UE, and also carry out power control and precoding, while keeping complexity at an acceptable level, which is difficult to attain as number of UEs increases. This can be solved by investigating user-centric and network-centric approaches for cell-free networks where only a limited number of APs in the vicinity of the user can serve such a user, but not all of them. Front-haul capacity relies mainly on the ability of CPU units to handle all transmissions from APs, and thus with utilizing multiple bands in case of NOMA CF-mMIMO with CA, it increases the overhead and complexity of processing of those signals at the CPU which requires further optimization. Deployment is considered one of the main challenges in CF-mMIMO system, so the authors in [22] studied a cell-free network without introducing costly hardware and cabling by means of radio strips [22], where the internal communications between APs are eliminated by integrating all cables between them and the antenna processing units (APUs) are all gathered into the same cable, giving simpler hardware with lower cost. Cost Efficiency for NOMA CF-mMIMO with CA tries to minimize the cost of implementing such a system, while keeping its performance at an acceptable level, and this may rely on a number of factors including: number of APs, number of clusters, cooperation level between APs, implementing a front-haul network able to withstand the large number of APs, power consumption of AP, and also number of aggregated bands. In [23], the authors provided a cost-analysis for CF-mMIMO system, and showed a unified model encompassing cell-free systems with variable number of antennas at each AP. This can be considered a good starting point for further analysis regarding cost efficiency of NOMA CF-mMIMO with CA.

REFERENCES

[1] T. L. Marzetta, "Noncooperative Cellular Wireless with Unlimited Numbers of Base Station Antennas," IEEE Transactions on Wireless Communications, vol. 9, pp. 3590-3600, November 2010.

[2] F. A. Pereira de Figueiredo, "An Overview of Massive MIMO for 5G and 6G," IEEE Latin America Transactions, vol. 20, pp. 931-940, June 2022.

[3] Y. Mao, B. Clerckx, "Beyond Dirty Paper Coding for Multi-Antenna Broadcast Channel With Partial CSIT: A Rate-Splitting Approach," IEEE Transactions on Communications, vol. 68, pp. 6775-6791, November 2020.

[4] H. Q. Ngo, E. G. Larsson, and T. L. Marzetta, "Aspects of favorable propagation in massive MIMO," 2014 22nd European Signal Processing Conference (EUSIPCO), Lisbon, Portugal, 2014, pp. 76-80.

[5] E. Anarakifirooz, and S. Loyka, "Favorable Propagation for Massive MIMO With Circular and Cylindrical Antenna Arrays," IEEE Wireless Communications Letters, vol. 11, pp. 458-462, March 2022.

[6] M. Ajmal, A. Siddiqa, B. Jeong, J. Seo, and D. Kim, "Cell-free massive multiple-input multiple-output challenges and opportunities: A survey," ICT Express, vol. 10, pp. 194-212, February 2024.

[7] M. Shafi, R. K. Jha, and S. Jain, "6G: Technology Evolution in Future Wireless Networks," IEEE Access, vol. 12, pp. 57548-57573, April 2024.

[8] H. Yahya, A. Ahmed, E. Alsusa, A. Al-Dweik, and Z. Ding, "Error Rate Analysis of NOMA: Principles, Survey and Future Directions," IEEE Open Journal of the Communications Society, vol. 4, pp. 1682-1727, July 2023.

[9] A.Jehan, and M. Zeeshan, "Comparative Performance Analysis of Code-Domain NOMA and Power-Domain NOMA," 2022 16th International Conference on Ubiquitous Information Management and Communication (IMCOM), Seoul, Republic of Korea, 03-05 January 2022, pp. 1-6.

[10] A. Apiyo, and J. Izydorczyk, "A Survey of NOMA-Aided Cell-Free Massive MIMO Systems," Electronics, 13(1), 231, January 2024.

[11] Y. Li, and G. A. Aruma Baduge, "NOMA-Aided Cell-Free Massive MIMO Systems," IEEE Wireless Communications Letters, vol. 7, pp. 950-953, Dec. 2018.

[12] T. Cui, C. Liu, P. Du, and R. Song, "Uplink Cell-Free Massive MIMO-NOMA Systems Based on Group-Level Successive Interference Cancellation," EURASIP Journal on Advances in Signal Processing, January 2022.

[13] R. Sayyari, J. Pourrostam, and M. J. M. Niya, "Cell-Free Massive MIMO System With an Adaptive Switching Algorithm Between Cooperative NOMA, Non-Cooperative NOMA, and OMA Modes," IEEE Access, vol. 9, pp. 149227-149239, November 2021.

[14] F. Rezaei, C. Tellambura, A. A. Tadaion, and A. R. Heidarpour, "Rate Analysis of Cell-Free Massive MIMO-NOMA With Three Linear Precoders," IEEE Transactions on Communications, vol. 68, pp. 3480-3494, June 2020.

[15] B. Chong, H. Lu, Y. Chen and L. Tian Qin, "Achievable Sum Rate Optimization on NOMA-aided Cell-Free Massive MIMO with Finite Block length Coding," June 2023.

[16] M. S. Ali, H. Tabassum, and E. Hossain, “Dynamic User Clustering and Power Allocation for Uplink and Downlink Non-Orthogonal Multiple Access (NOMA) Systems, ” IEEE Access, vol. 4, pp. 6325-6343, August 2016.
[17] R. Arshad, S. Baig, and S. Aslam, “User clustering in cell-free massive MIMO NOMA system: A learning based and user centric approach,” Alexandria Engineering Journal, vol. 90, pp. 183-196, March 2024.
[18] X. Han et al., “Flexible Spectrum Orchestration Of Carrier Aggregation For 5G-advanced,” in IEEE Communications Standards Magazine, vol. 7, pp. 68-74, December 2023.
[19] A. Zappone, D. López-Pérez, A. D. Domenico, N. Piovesan, and H. Bao, “Rate, Power, and Energy Efficiency Trade-Offs in Massive MIMO Systems With Carrier Aggregation,” IEEE Transactions on Green Communications and Networking, vol. 7, pp. 1342-1355, September 2023.
[20] O. Afolalu O, and N. Ventura, “Carrier aggregation-enabled non-orthogonal multiple access approach towards enhanced network performance in 5G Ultra-Dense Networks,” International Journal of Communication Systems, 2021.
[21] S. M. Kay, Fundamentals of Statistical Signal Processing: Estimation Theory, Englewood Cliffs, NJ: Prentice Hall, 1993.
[22] G. Interdonato, E. Björnson, and H. Q. Ngo, “Ubiquitous cell-free Massive MIMO communications,” J. Wireless Com. Network, August 2019.
[23] W. Jiang, and H. Schotten, “Cost-Effectiveness Analysis and Design of Cost-Efficient Cell-Free Massive MIMO Systems,” arXiv, June 2024.